Photonic Films

DOI: 10.1002/anie.201100446

Transfer of Preformed Three-Dimensional Photonic Crystals onto Dye-Sensitized Solar Cells**

*Agustín Mihi, Chunjie Zhang, and Paul V. Braun**

Photonic crystals are materials that exhibit periodicities in their refractive index on the order of the wavelength of light, and thus provide many interesting possibilities for "photon management".[1,2] Applications for photonic crystals include light bending, inhibition of spontaneous emission, and amplified photon absorption or emission.[3] A major limitation, however, for the incorporation of photonic crystals, in particular self-assembled three-dimensional photonic crystals, in optoelectronic devices are incompatibilities between the fabrication routes for the photonic structures and the active device. Most notably, the ideal substrate for the self-assembly of colloidal photonic crystals is a planar, nonporous, and chemically homogeneous surface, yet most active devices have rough surfaces, are chemically heterogeneous, and are often porous.

Three-dimensional photonic colloidal crystals are of particular interest for enhancing light harvesting in dye-sensitized solar cells (DSSCs) because these crystals can both be porous and significantly enhance light–matter interactions. Diffraction, dielectric mirror effects, and resonant modes are some of the phenomena that are exhibited by photonic crystals and can greatly enhance the effective light optical path within the active layer.[4–6] In DSSCs, the light absorption takes place in an organic dye adsorbed onto a porous conductive network. The overall efficiency is limited because in most cases the dye does not exhibit a strong optical absorption towards the red part of the visible spectrum.[7] This limitation is particularly dramatic when the typical titania matrix is substituted by a material with improved electron mobility but lower surface area, such as ZnO nanowires (NWs).[8] Increasing the light–matter interaction, for example through the use of a porous photonic crystal coupled to the working electrode, would increase the overall efficiency. Artificial opals are good candidates for this role because of their inherent porosity, which allows the liquid electrolyte present in DSSCs to regenerate the oxidized dye. However, growth of a photonic crystal on a rough and porous DSSC working electrode is nearly impossible. Additional issues arise if higher-refractive-index photonic crystals, which are formed by using a colloidal crystal as a template for a high-dielectric-contrast material such as titanium oxide or silicon, are desired because of their potential to exhibit wider or even full photonic bandgaps.[9,10] The inversion steps used to form such structures will clog the pores of the DSSC electrode, thus preventing adsorption of the sensitizing dye. Previous attempts to form photonic crystals on DSSCs include spin-coating of colloidal crystals,[11] use of an intermediate polymer layer that coats the titania layer,[12] and substitution of the nanocrystalline titania layer with a mesoporous film to provide better surface properties for opal growth.[13] However, these methods provide photonic crystal films with low optical quality compared with what can be achieved on flat substrates, thus reducing the benefits of the optical coupling between the photonic structure and the photovoltaic device.

Herein we demonstrate the general concept of transferring preformed 3D photonic crystals onto various substrates, and in particular, the coupling of preformed photonic crystals with independently processed porous DSSCs. We fabricated three-dimensional colloidal, inverse opal silicon, and inverse opal titania photonic crystals, embedded them in a polycarbonate matrix, and transferred them onto several different types of porous electrodes used in DSSCs. The excellent optical properties of the photonic crystal films are maintained and an enhancement in the efficiency of the DSSCs is observed.

The key step in the fabrication and transfer of the preformed photonic films is the infiltration of the photonic structure with a polycarbonate (PC) matrix that provides mechanical stability to the film after it is released from its original substrate yet can be cleanly thermally removed. This polymer has been used previously to enable the formation of free-standing flexible porous inorganic one-dimensional Bragg stacks.[14] The first step is the growth of a silica colloidal crystal by evaporation-induced self-assembly on an oxidized silicon substrate (Figure 1a).[15] The oxide layer acts as a sacrificial release layer when the substrate is immersed in hydrofluoric acid. The release step is only necessary for the transfer of inverted photonic crystals (e.g., Si or TiO_2). If desired, the colloidal crystals are subsequently infiltrated with 20 nm of TiO_2 ($n = 2.4$) by atomic layer deposition (ALD)[16] or 48 nm of amorphous silicon ($n = 3.5$) by chemical vapor deposition (CVD;[17] Figure 1b). The silica colloidal crystals,

[*] Dr. A. Mihi, C. Zhang, Prof. P. V. Braun
Department of Materials Science and Engineering
Frederick Seitz Materials Research Laboratory
Beckman Institute for Advanced Science and Technology
University of Illinois at Urbana-Champaign
Urbana, IL 61801 (USA)
Fax: (+1) 217-333-2736
E-mail: pbraun@illinois.edu
Homepage: http://braungroup.beckman.illinois.edu/

[**] This work was supported by a Department of Energy Basic Energy Sciences, Office of Science grant through the "Light-Material Interactions in Energy Conversion" Energy Frontier Research Center under contract number DE-SC0001293. A.M. thanks the Beckman Institute for a postdoctoral fellowship. This research was carried out in part in the Center for Microanalysis of Materials, UIUC, which is partially supported by the U.S. Department of Energy under grants DE-FG02-07ER46453 and DE-FG02-07ER46471.

Supporting information for this article is available on the WWW under http://dx.doi.org/10.1002/anie.201100446.

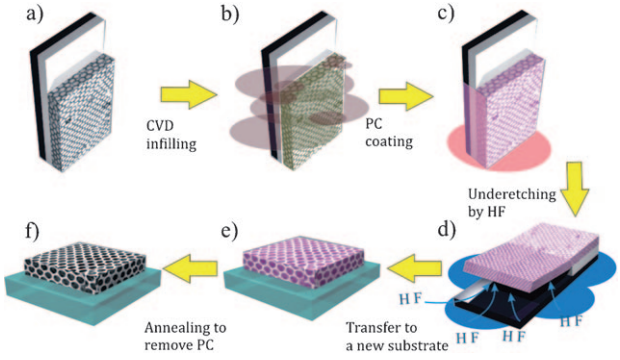

Figure 1. Fabrication and transfer of preformed photonic films. a) A colloidal crystal is grown on a silica-coated silicon substrate. b) The porous opal is infilled with TiO_2 or Si by gas-phase deposition. c) The photonic crystal film is dipped in a polycarbonate (PC) solution. d) The PC-infilled photonic film is released through HF etching and the silica template is removed. e) The preformed photonic crystal film is transferred to the receiving substrate. f) An inverse photonic structure is obtained after removal of the polymer.

titania–silica, or silicon–silica structures were then dipped in polycarbonate (PC; 5% w/w in chloroform) and dried for 3 hours at 65 °C. After the PC infiltration, the bare silica opals spontaneously peeled off from the substrate when immersed in deionized water. The other films were partially released from the substrate when immersed overnight in 5% HF in water (Figure 1d), and remained bound to the substrate at only the edges of the film (Figure 2a). The original silica

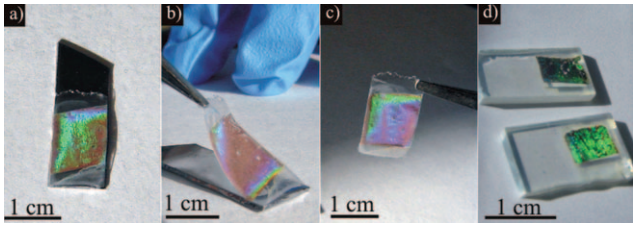

Figure 2. Photographs of stages of the transfer process of a silicon photonic crystal. a) The silicon photonic film on its original substrate after underetching with HF. b) The film is gently peeled from the substrate with tweezers. c) The preformed film is ready to be deposited onto any substrate. d) Inverse Si opals on dye sensitized ZnO NW electrodes after calcination at 500 °C for 2 h.

template was also removed by the HF. The films were then rinsed with ethanol and dried with nitrogen. The photonic films were then transferred to a new substrate by adding a drop of binder (5% w/w PC in chloroform) on the new surface and placing the film on top (Figure 1e). Heating to 500 °C removes the PC and binds the photonic crystal to the new substrate (Figure 1f). Images taken though the process of transferring a preformed silicon photonic crystal onto a ZnO NW working electrode are shown in Figure 2.

Preformed photonic films were transferred onto both nc-TiO_2 (nc = nanocrystalline) and ZnO NW electrodes to create photonically enhanced DSSCs. Scanning electron microscopy (SEM) images of the resulting electrodes are shown in Figure 3. Silica (Figure 3a), inverse titania (Figure 3b), and

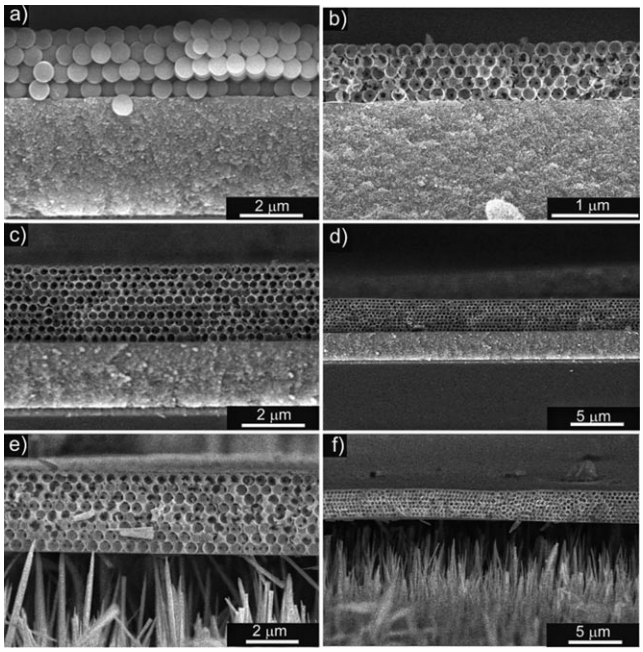

Figure 3. Cross-sectional SEM images. a) 420 nm diameter silica colloidal crystal on a 5 μm thick nc-TiO_2 layer. b) 420 nm diameter titania inverse photonic crystal on a 5 μm thick nc-TiO_2 layer. c,d) 500 nm diameter inverse silicon photonic crystals on a 5 μm thick nc-TiO_2 layer at different magnifications. e,f) 500 nm diameter inverse silicon photonic crystal on a substrate covered with 10 μm long ZnO nanowires (150–200 nm diameter) at different magnifications.

inverse silicon (Figure 3c,d) opals were deposited onto nc-TiO_2 layers. An inverse silicon opal was also deposited onto a 10 micrometer thick ZnO nanowire array (Figure 3e,f). The samples exhibit large crack-free regions because of the use of preheated silica beads as templates,[18] therefore improving the final optical quality of the resulting structures. The primary problem observed was delamination of the photonic films from the receiving substrates (in particular the ZnO NW substrate). To minimize delamination, binders including water, polyvinyl alcohol, and PC solutions were investigated. Delamination was rarely observed when the PC binder was used.

The electrode/three-dimensional photonic structure combinations exhibit excellent optical properties, as can be observed in the reflectance spectra shown in Figure 4. The reflectance spectra of the silica colloidal crystal on its native silicon substrate, the bare nc-TiO_2 electrode, and the electrode containing the transferred photonic film are shown in Figure 4a–c. The reflectance peak that arises from the photonic pseudogap of the artificial opal maintains its original intensity, and the secondary lobes are convoluted with the Fabry–Perot fringes produced by the finite thickness of the titania film. Figure 4d corresponds to the reflectance spectrum of an inverse titania deposited onto a nc-TiO_2 electrode. The inverse titania opal is of particular interest because of the compatibility of this photonic structure and the TiO_2 backbone of the light-harvesting electrode in a DSSC. The primary limitations of the incorporation of these structures into solar cells are the difficulties of growing high-quality artificial opals

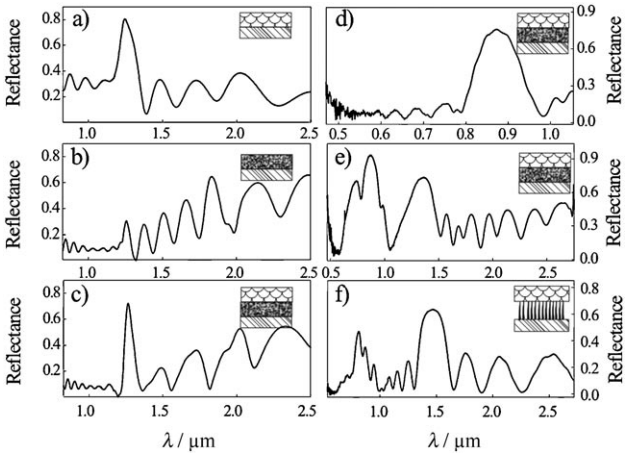

Figure 4. Specular reflectance spectra at different stages of the transferring process: a) the starting silica colloidal crystal on a silicon substrate (500 nm diameter colloids; inset: bare opal/silicon). b) 5 μm thick nc-TiO_2 layer on FTO-coated glass (inset: nc-TiO2/FTO-coated glass). c) silica colloidal crystal transferred onto the 5 μm thick nc-TiO_2 layer. The spectra from different photonic crystals on two kinds of electrodes are also shown (inset: bare opal/nc-TiO2/FTO-coated glass). d) Titania inverse photonic crystal (420 nm colloidal template) on a 5 μm thick nc-TiO_2 layer and a inverse silicon photonic crystal (500 nm diameter colloidal template; inset: inverse TiO2 opal/nc-TiO2 layer/FTO-coated glass), on a e) 5 μm thick nc-TiO_2 layer (inset:inverse Si opal/nc-TiO2/FTO-coated glass) and f) 10 μm long ZnO nanowires (inset: inverse Si opal/ZnO NW array/FTO-coated glass).The insets in each section represent the structure from which the spectra were taken. FTO = fluorine-doped tin oxide.

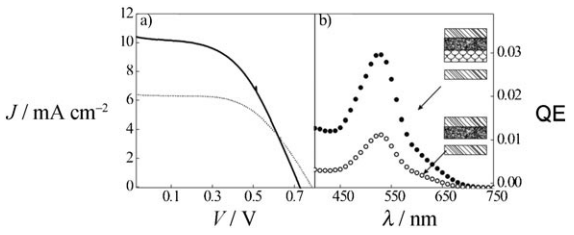

Figure 5. a) Current–voltage curve (AM 1.5 illumination 112 mW cm^{-2}; active area 0.25 cm^2) and b) quantum efficiency (monochromator slit opening 1.5 mm) plots for control (gray dotted line/open circles) and inverse silicon coupled (black solid line/filled circles) DSSCs. The values for the reference cell are $J_{sc} = 6.3$ mA cm^{-2}, $V_{oc} = 0.78$ V, $\eta = 2.33\,\%$, $FF = 0.52$. The values for the photonic crystal coupled cell are $J_{sc} = 10.26$ mA cm^{-2}, $V_{oc} = 0.73$ V, $\eta = 3.2\,\%$, $FF = 0.48$. QE = quantum eficiency.

on the porous electrodes, and the risk of clogging the porosity of the titania (the support for the sensitizing dye) during the templating process. By transferring a preformed titania photonic crystal, both of these issues are overcome. This approach enables even the use of silicon inverse opals with a very high refractive-index contrast for the first time in a DSSC. Figure 4e,f shows the reflectance spectra of inverse silicon photonic crystals deposited onto a nc-TiO_2 layer (Figure 4e) and a ZnO NW array (Figure 4f). Two main features can be observed in both systems; the peak at higher wavelengths corresponds to the photonic pseudogap that arises from the diffraction from the (111) planes and a set of peaks at higher energy where the complete photonic bandgap is expected (Figure SI1 in the Supporting Information). The use of a preformed silicon photonic crystals to enhance photon absorption is particularly attractive for ZnO-NW-based DSSCs. Because the surface area, and thus dye loading, of these electrodes is low, methods to enhance the interaction of light with the structure are of great interest.

To test the performance enhancement provided by the transferred photonic films in a real device, nc-TiO_2 and ZnO-NW-based DSSCs were assembled with and without inverse silicon photonic crystals. The cells were otherwise fabricated by following standard procedures.[19] Characterization of the solar cells with and without inverse silicon photonic crystal films are summarized in Figure 5. The power efficiency of the solar cell with photonic crystal ($\eta = 3.2\,\%$, fill factor (FF) = 0.48) is 39% better than a reference cells ($\eta = 2.3\,\%$, FF = 0.52; Figure 5a). The external quantum efficiency of both devices is presented in Figure 5b; higher photocurrents are observed for the cell with the photonic film. Similarly, the ZnO NW DSSC cells containing the photonic structure exhibit higher efficiency values ($\eta = 0.679\,\%$, $FF = 0.353$) than those without ($\eta = 0.586\,\%$, $FF = 0.286$). Because of the liquid electrolyte ($n = 1.33$) infilling the solar cell, the refractive index contrast in the inverse silicon photonic crystal is reduced, hence there is not a complete photonic bandgap (Figure SI1), however, the photonic band structure at this range still presents a large pseudogap, bands with very flat dispersion relations, and diffraction channels that can enhance the interaction between incoming light and the absorbing material. To evaluate the optical effect of coupling the inverse silicon structure to the nc-TiO_2 electrode, the reflectance spectra from liquid-filled cells with and without an inverse silicon photonic crystal film were measured (Figure SI2). Strong reflectance was observed from the cell containing the photonic crystal, thus demonstrating that the photonic crystal can be used to redirect light towards the working electrode.

In conclusion, we have demonstrated an approach for coupling preformed direct or inverse three-dimensional photonic crystals of different materials with a diverse set of surfaces. In particular, we have demonstrated enhanced light trapping in DSSCs by coupling a porous photonic crystal film to both nc-TiO_2 and ZnO NW DSSC electrodes. The transferred photonic films exhibit high optical quality, and the transfer process does not damage or disrupt the porosity of the DSSC electrodes. The films increase the efficiency of a model titania DSSC system from 2.3% to 3.2%. Our approach decouples the processing of the photonic structure from the processing of the DSSC electrode, and thus allows the incorporation of inverse silicon photonic crystals in these devices. The ability to transfer preformed silicon photonic structures into arbitrary substrates may enable the coupling of structures containing unique photonic properties such as full band gaps[6] or superprism effects[20] onto a wide variety of devices.

Experimental Section

Oxide-coated silicon substrates: Silicon substrates with two kinds of sacrificial oxide layer were employed with similar results: 10 nm of aluminum oxide by ALD (Savannah 100, Cambridge NanoTech) or 1 μm of silica (MontCo Silicon Technologies).

TiO_2 and ZnO NW electrodes: 5–7 μm nc-TiO_2 films were deposited using squeegee of a titania paste (Solaronix, Ti-Nanoxide HT) on FTO substrates (Hartford Glass Co.) and annealing at 450 °C for 30 min. 10 μm ZnO Nanowires were grown on FTO glass using a hydrothermal method as described elsewhere.[21] In brief, the substrates were immersed in an aqueous dispersion of zinc hexahydrate and hexamethylamine for 12 h at 90 °C, the solution was replaced every three hours.

Colloidal crystals were grown from 420 and 500 nm diameter silica spheres synthesized by the Stöber method followed by several regrowths. The spheres were heat-treated for 10 h at 600 °C to avoid shrinkage of the films during the templating process. Substrates that were cleaned with Piranha solution were placed at a 20° angle in a 20 mL scintillation vial (Fisher) with 4 g of colloidal dispersion (2–3 % w/w in ethanol). The vials were placed in an incubator (Fisher, Isotemp 125D) at 37 °C overnight. In the case of silicon inverse opals, the colloidal films were coated with 5 nm of alumina (ALD) to maximize the width of the photonic bandgap.[17]

TiO_2 coatings were deposited through ALD under the following conditions: the N_2 flow was set at 20 sccm, and the opening times of the water and titanium tetraisopropoxide ($C_{12}H_{28}O_4Ti$) valves were set to 0.015 s and 0.065 s, respectively. The deposition chamber temperature was held at 200 °C. After 1000 cycles, the coating on the silica colloidal crystal was 18–20 nm. Samples were annealed at 500 °C for 2 h to crystallize the titania into the anatase phase.

Silicon coatings were performed using a CVD system with disilane (Si_2H_6, 98 %, Gelest) as a silicon source. 500 nm diameter silica colloidal crystals were coated with 48 nm of amorphous Si through one deposition cycle (50 mbar, 3 h, 350 °C, heating rate 8 °C min^{-1}). Reactive ion etching (1 min, 70 W, gasses SF_6 and O_2 20 sccm, 50 mTorr chamber pressure) was performed afterwards to expose the silica spheres.

Lift-off process: Polycarbonate (Makrolon) coating was carried out by immersing the samples in a 5 % w/w PC in chloroform followed by drying in oven at 65 °C for 3 hours. Bare silica opals would peel off spontaneously, titania-coated and silicon-coated films were immersed overnight in HF (5 % w/w in water) to release them from the substrate and remove the silica template.

Transfer: Polycarbonate-coated photonic films were transferred onto new substrates using a drop of a 5 % w/w PC in chloroform and placing the film with the PC-coated side in contact with the binder to create a single polymer layer.

Dye-sensitized solar cells were assembled using nc-TiO_2 and ZnO NW on FTO-coated glass electrodes with and without transferred inverse silicon photonic crystals, dyed overnight with N719 in ethanol (one hour in the case of ZnO NWs), assembled against Pt-coated FTO (Pt catalyst, Solaronix), and filled with a liquid electrolyte (iodine: 100 mM, lithium iodide: 100 mM, tetrabutylammonium iodide: 600 mM, tert-butylpyridine: 500 mM, in acetonitrile).

Characterization: Scanning electron microscopy (Hitachi S-4700 SEM) samples were gold–palladium-coated prior to imaging; reflectance spectra were measured using a Bruker Hyperion microscope coupled into a Bruker Vertex 70 FTIR spectrometer equipped with a 10×, 0.25 NA objective with a 3.75 mm spatial mask. External quantum efficiency was measured with an OL 750 spectroradiometer (Optronic Labs.), with a 1.5 mm slit aperture in the monochromator and under white-light bias (5 A lamp current). Current–voltage characterization of the solar cells was carried out at room temperature using a DC source meter (model 2400, Keithley) operated by LabVIEW5, and a 1000 W full-spectrum solar simulator (model 91192, 4×4 inch source diameter, ±4 collimation, Oriel) equipped with AM 1.5 direct filters. The input power of light from the solar simulator was measured with a power meter (model 70260, Newport) and a broadband detector (model 70268, Newport) at the point where the top surface of the sample was placed.

Received: January 18, 2011
Published online: May 9, 2011

Keywords: colloidal crystals · nanostructures · photonic crystals · solar cells

[1] S. John, *Phys. Rev. Lett.* **1987**, *58*, 2486.
[2] E. Yablonovitch, *Phys. Rev. Lett.* **1987**, *58*, 2059.
[3] K. A. Arpin, A. Mihi, H. T. Johnson, A. J. Baca, J. A. Rogers, J. A. Lewis, P. V. Braun, *Adv. Mater.* **2010**, *22*, 1084.
[4] A. Mihi, F. J. Lopez-Alcaraz, H. Miguez, *Appl. Phys. Lett.* **2006**, *88*, 193110.
[5] S. Nishimura, N. Abrams, B. A. Lewis, L. I. Halaoui, T. E. Mallouk, K. D. Benkstein, J. van de Lagemaat, A. J. Frank, *J. Am. Chem. Soc.* **2003**, *125*, 6306.
[6] P. Bermel, C. Luo, L. Zeng, L. C. Kimerling, J. D. Joannopoulos, *Opt. Express* **2007**, *15*, 16986.
[7] B. O'Regan, M. Gratzel, *Nature* **1991**, *353*, 737.
[8] M. Law, L. E. Greene, J. C. Johnson, R. Saykally, P. D. Yang, *Nat. Mater.* **2005**, *4*, 455.
[9] R. C. Schroden, M. Al-Daous, C. F. Blanford, A. Stein, *Chem. Mater.* **2002**, *14*, 3305.
[10] J. Wijnhoven, L. Bechger, W. L. Vos, *Chem. Mater.* **2001**, *13*, 4486.
[11] A. Mihi, M. E. Calvo, J. A. Anta, H. Miguez, *J. Phys. Chem. C* **2008**, *112*, 13.
[12] S. H. A. Lee, N. M. Abrams, P. G. Hoertz, G. D. Barber, L. I. Halaoui, T. E. Mallouk, *J. Phys. Chem. B* **2008**, *112*, 14415.
[13] S. Guldin, S. Huttner, M. Kolle, M. E. Welland, P. Muller-Buschbaum, R. H. Friend, U. Steiner, N. Tetreault, *Nano Lett.* **2010**, *10*, 2303.
[14] M. E. Calvo, O. S. Sobrado, G. Lozano, H. Miguez, *J. Mater. Chem.* **2009**, *19*, 3144.
[15] P. Jiang, J. F. Bertone, K. S. Hwang, V. L. Colvin, *Chem. Mater.* **1999**, *11*, 2132.
[16] J. S. King, E. Graugnard, C. J. Summers, *Adv. Mater.* **2005**, *17*, 1010.
[17] S. A. Rinne, F. Garcia-Santamaria, P. V. Braun, *Nat. Photonics* **2008**, *2*, 52.
[18] A. A. Chabanov, Y. Jun, D. J. Norris, *Appl. Phys. Lett.* **2004**, *84*, 3573.
[19] Q. Wang, S. Ito, M. Gratzel, F. Fabregat-Santiago, I. Mora-Sero, J. Bisquert, T. Bessho, H. Imai, *J. Phys. Chem. B* **2006**, *110*, 25210.
[20] H. Kosaka, T. Kawashima, A. Tomita, M. Notomi, T. Tamamura, T. Sato, S. Kawakami, *Phys. Rev. B* **1998**, *58*, R10096.
[21] L. E. Greene, M. Law, J. Goldberger, F. Kim, J. C. Johnson, Y. F. Zhang, R. J. Saykally, P. D. Yang, *Angew. Chem.* **2003**, *115*, 3139; *Angew. Chem. Int. Ed.* **2003**, *42*, 3031.

